The Ligand-to-Metal Charge Transfer Excited State of $[Re(dmpe)_3]^{2+}$

Tayliz M. Rodriguez[†], Mawuli Deegbey[‡], Elena Jakubikova[‡], Jillian L. Dempsey[†]

[†]Department of Chemistry, University of North Carolina at Chapel Hill, Chapel Hill, North Carolina 27599-3290, United States

[‡]Department of Chemistry, North Carolina State University, Raleigh, North Carolina 27695, United States

*Corresponding author: dempseyj@email.unc.edu

Abstract

The ligand-to-metal charge transfer (LMCT) transitions of $[Re(dmpe)_3]^{2+}$ (dmpe = bis-1,2-(dimethylphosphino)ethane) were interrogated using UV/Vis absorbance spectroscopy, photoluminescence spectroscopy, and time-dependent density functional theory. The solvent dependence of the lowest energy charge transfer transition was quantified; no solvatochromism was observed. TD-DFT calculations reveal the dominant LMCT transition is highly symmetric and delocalized involving all phopshine ligand donors in the charge transfer, providing an understanding for the absence of solvatochromism of $[Re(dmpe)_3]^{2+}$.

Introduction

Transition metal complexes with long-lived charge transfer excited states find broad applications as chromophores and photosensitizers (Kalyanasundaram 1982; Esswein and Nocera 2007; Prier et al. 2013). Some transition metal complex excited states undergo light-driven redox reactivity rendering them useful for driving chemical transformations such as photoredox catalysts or enabling energy storage reactions. The majority of useful photochemistry accessed from transition metal complexes has been accomplished with complexes that possess metal-to-ligand charge transfer (MLCT) excited states (Prier et al. 2013). In contrast to the number of known complexes with MLCT excited states, examples of coordination complexes with ligand-to-metal charge transfer (LMCT) excited states are relatively scarce. LMCT transitions require an oxidizable donor ligand and an electron deficient metal center as excitation to an LMCT state results in the formal reduction of the metal center and oxidation of the ligand to its radical cation. The majority of coordination complexes with LMCT transitions in the visible region have been reported for d^0 complexes (Larsen and Wenger 2018; Paulson and Sullivan 1992; Pfenning et al. 1989; Williams and Korolev 1995; Choing et al. 2015; Zhang et al. 2016; Romain et al. 2014; Tonks et al. 2012), as these complexes provide low-energy vacant metal based acceptor orbitals. Examples of d^5, d^6, and f^0 complexes with LMCT excited states have also been reported (Williams et al. 1996; Foo Lee and Jon 1994; Bandy et al. 1988; Kunkley and Vogler 2001; Qiao and Schelter 2018; Yam et al. 1996; Kanso et al. 2020; Vogler and Kunkley 1981; Kaul et al. 2019; Chábera et a. Nature; Alexander and Gray 1968; Adams et al. 2015; Pal et al. 2018; Yam et al. 2001a). In general, orbitals of the donor ligands involved in charge transfer transitions are poorly understood. Experimental and computational studies that probe the electronic structures of coordination complexes with LMCT excited states are necessary to realize their photochemical applications.

Towards this, we describe here studies to further elucidate the electronic structure of $[Re(dmpe)_3]^{2+}$ (dmpe = bis-1,2-(dimethylphosphino)ethane) (Figure 1).

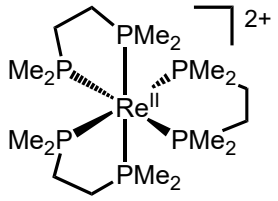

Figure 1: Structure of $[Re(dmpe)_3]^{2+}$

Re(II) and Tc(II) complexes of the formula $[M(dmpe)_3]^{2+}$ (M = Re, Tc) are the most studied d^5 complexes with emissive LMCT excited states (Foo Lee and Jon 1994; Kirchhoff et al. 1997; Del Negro et al. 2006; Chatterjee et al. 2013; Adams et al. 2015). These complexes have attracted attention due to their highly oxidizing excited states ($E_{1/2}(Re^{2+*}/Re^{+})$ = 2.20 V vs Fc/Fc^{+} in CH_3CN), which are capable of oxidizing relatively inert organic and inorganic substrates (Del Negro et al. 2006). Analogues of the Re(II) complex incorporating a series of chelating phosphine ligands with varying linkers and pendant groups have recently been reported; substitution with 1,2-bis(dimethylphosphino)benzene (dpbz) and bis-(diphenylphosphino)methane (dppm) yields complexes with even more highly oxidizing excited-state potentials (Adams et al. 2015). Previous theoretical work assigned the lowest energy absorption of $[Re(dmpe)_3]^{2+}$ as a spin-allowed LMCT doublet-doublet transition from σ(P) to dπ(Re), but a complete calculated electronic absorbance spectrum has not been reported and compared to experimental data, nor has the solvatochromism of this charge transfer transition been studied (Del Negro et al. 2006). Here, we expand on previous computational studies to interrogate the electronic structure of $[Re(dmpe)_3]^{2+}$ and further investigate the charge transfer nature by examining the solvent dependence of the LMCT transition. Charge transfer transitions can lead to changes in dipole moments between the ground and excited states, and the stabilization of these states by solvent is related to solvent polarity. Since solvents of higher polarity can more effectively stabilize the charge transfer and, in turn, shift absorption and emission features to lower energies in an effect known as solvatochromism, absorption and emission measurements made in solvents of varying polarities can be used to support a charge transfer transition (Marini et al. 2010). Experimentally and computationally, we find an unexpected absence of solvatochromism for the low energy LMCT transition, but understand this phenomenon by visualizing the Mulliken populations of the donor and acceptor orbitals and by calculating the associated change in dipole moment. These calculations reveal a high degree of symmetry in the key charge transfer transition.

Results and Discussion

$[Re(dmpe)_3][BAr^F{}_4]_2$ ($BAr^F{}_4$ = tetrakis[3,5-bis(trifluoromethyl)phenyl]borate) was prepared through modification of a literature procedure (Adams et al. 2015). $[Re(dmpe)_3][BAr^F{}_4]$ is first synthesized from the Re(V) oxo complex $[ReO_2(py)_4]Cl$ followed by salt metathesis with

$NaBAr^F_4$. The Re(I) complex is chemically oxidized with $[Ph_3C][BAr^F_4]$ in CH_3CN to yield $[Re(dmpe)_3][BAr^F_4]_2$.

The absorption and emission spectra of $[Re(dmpe)_3]^{2+}$ in CH_3CN are shown in Figure 2. The UV/Vis absorbance spectra of $[Re(dmpe)_3]^{2+}$ possesses two features in the visible region (λ_{max} = 416 and 527 nm), where the major feature at low-energy (λ_{max} = 527 nm; ε = 1348 $M^{-1}cm^{-1}$) has previously been assigned as a $P(\sigma) \rightarrow Re(d\pi)$ LMCT transition (Foo Lee and Jon 1994; Del Negro et al. 2006). Assignments of additional transitions are discussed below. $[Re(dmpe)_3]^{2+}$ exhibits strong emission in CH_3CN at room temperature centered at 605 nm, with a low-energy broad feature from 750 – 900 nm. The emission profile is independent of excitation wavelength suggesting the source of emission originates from the lowest-energy LMCT transition. In addition, the lifetime of the strong (605 nm) and weak band (750 – 900 nm) are the same within error (τ = 11.5 and 11.3 ns, respectively).

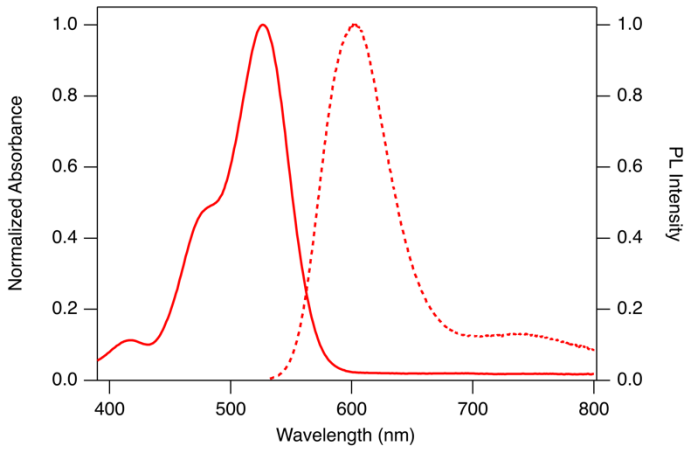

Figure 2: Absorption (solid line) and photoluminescence emission (dashed line) spectra of $[Re(dmpe)_3](BAr^F)_2$ in CH_3CN.

Previous studies have utilized time-dependent density functional theory (TD-DFT) to interrogate the nature of the optical transitions of $[Re(dmpe)_3]^{2+}$ using population analysis of the orbital contributions. As noted above, the lowest energy transition has been assigned as predominantly LMCT in character, with a transition from a σ(P) orbital to a dπ(Re) orbital (Del Negro et al. 2006). We expanded previous computational work in order to derive electronic spectra and construct orbital representations that further describe the observed optical transitions and charge transfer nature of $[Re(dmpe)_3]^{2+}$. Unrestricted open-shell TD-B3LYP (Becke 1988, 1993; Casida et al. 1998) with the 6-311G* (Krishnan et al. 1980; McLean and Chandler 1980) basis set for the ligand atoms (C, H and P) and SDD effective core potential with the associated basis set (Dolg et al. 1987) for Re was used to assign the optical transitions of $[Re(dmpe)_3]^{2+}$. The electronic spectra was predicted implicitly in acetonitrile using the polarizable continuum solvation model (PCM, Figure 3A) (Scalmani and Frisch 2010). The calculated lowest-energy LMCT transition (2.56 eV) has a relatively high oscillator strength (0.021) and corresponds to a spin-allowed doublet-doublet transition. This excitation involves transition of electron density from a

predominantly ligand-based (dmpe) molecular orbital (MO 127β) to a metal-based orbital (MO 130β), which is consistent with previous reports (Figure 3B) (Chatterjee et al. 2013). The calculated transition energy of 2.56 eV (490 nm) is in fair agreement with the experimental absorption energy of 2.35 eV (527 nm) and is similar to the previously calculated transition at 2.63 eV (Del Negro et al. 2006). The closer energy match is due to the change in basis sets for the ligand and metal atoms (6-311G* and SDD, respectively) in this work, and the included solvation. Two other LMCT states; 2.88 eV (MO 126β to 130β) and 2.93 eV (MO 125β to 130β) with low oscillator strength are also predicted. In addition, two low-energy d-d transitions from MO 129β and 128β to 130β are predicted to be about 0.4 eV above the ground state with no oscillator strength. The percent contribution of the orbital fragments involved in the vertical transitions was determined through Mulliken population analysis using the AOMix software (Gorelsky). The lowest-energy LMCT transition (127β→130β) involves a transition from an orbital with 82% dmpe character (ligand-based) to a metal d-orbital of 77% Re character. Of the 82% ligand-based character, approximately 51% is comprised of phosphorus (σ(P)).

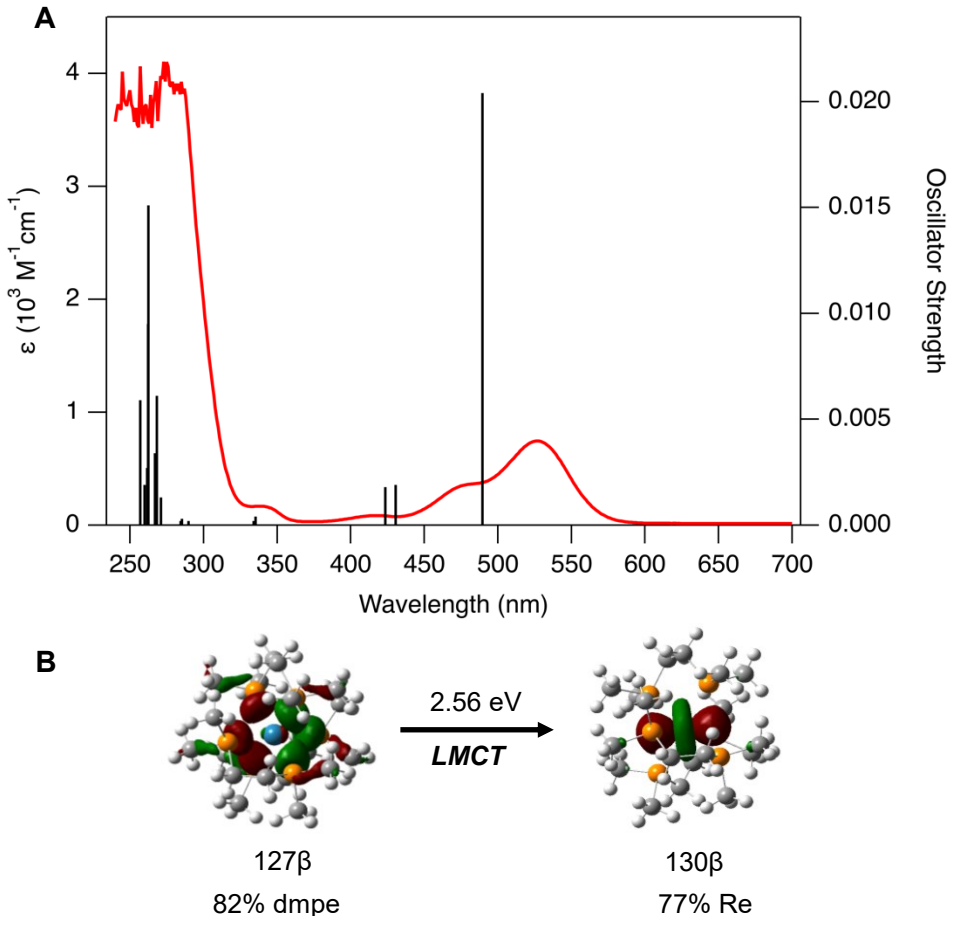

Figure 3: A) Experimental electronic spectra (red) and TD-DFT predicted vertical transitions (vertical lines) of $[Re(dmpe)_3]^{2+}$ in CH_3CN (PCM solvation). B) The donor and acceptor orbitals contributing to the lowest energy vertical transition, and dominant LMCT transition, are shown.

When excitation shifts electron density from one part of the molecule to another, the excited state typically has a distinct dipole moment in comparison to the ground state. Different solvents can stabilize ground and excited states differently based on their polarity, and thus the energy of the charge transfer excitation can depend on the solvent properties in a phenomenon known as solvatochromism (Chen and Meyer 1998). For this reason, the charge transfer nature of the transition can be quantified by the shifts in absorption and emission maximum as a function of solvent polarity (Chen and Meyer 1998; Hush and Reimers 2006). In general, with an increase in solvent polarity, a red-shift (spectral shift to longer wavelength) is observed when the excited state dipole moment of a compound is larger than the ground state dipole moment; and vice-versa for a blue-shift (Reichardt 1994). Solvatochromism in absorption and/or emission features have previously been used to support LMCT assignments (Shepherd et al. 1984; Paulson et al. 1992; Loukova et al. 2007a, 2016).

While theory supports assignment of the lowest-energy LMCT state of $[Re(dmpe)_3]^{2+}$ to be charge transfer in nature, absorbance spectra of $[Re(dmpe)_3]^{2+}$ recorded in solvents of varying polarity exhibit a minimal red shift of the LMCT transition, ranging from λ_{max} = 526 nm in CH_2Cl_2 to 531 nm in DMF (Figure 4). The slight bathochromic (red) shift of this transition exhibits no correspondence to the solvent polarity suggesting the excited state is not stabilized (or destabilized) by increased solvent polarity. The shifts are extremely small and inconsistent with solvatochromism generally observed for complexes with charge transfer excited states (Table 1). For example, solvents of increasing polarity yield a red-shift of the low-energy LMCT absorption bands as well as larger Stokes shifts for d^0 bridged zirconocene dichloride complexes. These complexes exhibit significant shifts in the absorption bands from 350 to 315 nm in solvents of high polarity, which supports the charge transfer nature of the transition and suggests stabilization of the excited state in polar solvents (Loukova et al. 2007). Complexes with metal-to-ligand charge transfer (MLCT) excited states also have large solvatochromic shifts in solvents of varying polarity. For instance, the Re(I) carbonyl complex *fac*-$Re(bpy)(CO)_3Ph$ exhibits negative solvatochromism; where the max absorption blue-shifts by nearly 40 nm in increasingly polar solvents (Sullivan 1989). On the other hand, the absence of solvatochromism has been observed for a Zr(IV) homoleptic photosensitizer with phosphorescent LMCT excited states. The lack of solvatochromism in this complex is attributed to an excited state delocalized over all ligands with a small change in dipole moment upon excitation (Zhang et al. 2020).

To further interrogate the solvent-independent photophysics observed experimentally, electronic spectra of $[Re(dmpe)_3]^{2+}$ were computed using TD-DFT and PCM solvation in CH_3CN, CH_2Cl_2, THF, and DMF and compared to experimental spectra. The calculated absorption spectra of $[Re(dmpe)_3]^{2+}$ in various solvents are shown in Figure 5 (additional comparison shown in Figure S1). These four simulated absorption spectra all exhibit two bands: one main band at ca. 485 nm and the other at ca. 432 nm, similar to the experimental spectra (Figure 4). As in the experimental spectra, no meaningful differences are observed in the position and shape of the absorption spectra band as the solvent is changed. Next, geometry optimization was performed on the lowest energy LMCT state using TD-DFT in CH_3CN. This was carried out to obtain the emission energy and

compare the geometrical parameters of the ground and lowest energy LMCT states (see Table S3 in ESI). The calculated emission energy, 2.31 eV (537 nm) obtained is ~0.26 eV higher than the experimental data, 2.05 eV (605 nm). A similar error is obtained with the absorption energy: a difference of ~0.21 eV between the calculated (2.56 eV) and experimental (2.35 eV) absorption energies. Thus, the calculated emission energy is in fair agreement with experiment. Comparison of the bond lengths and bond angles between the ground state and the lowest energy LMCT state shows a small deviation in these parameters. The average Re-P bond length shortens by ~ 0.03 Å upon excitation, and the P-Re-P bite angle decreases by ~1.41° . These data indicate that there is only a small change in the electronic structure upon excitation from the ground state to the lowest energy LMCT state.

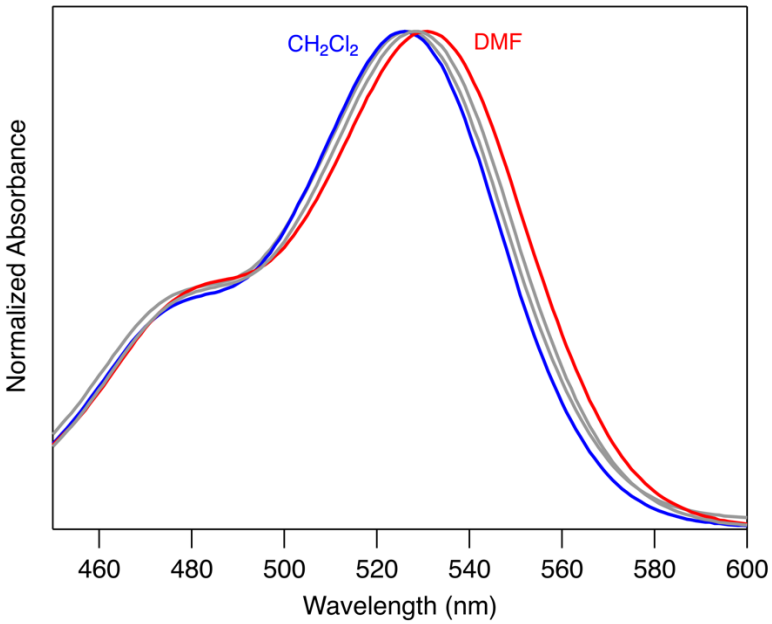

Figure 4: Normalized UV/Vis absorbance spectra of 1 mM solution of $[Re(dmpe)_3]^{2+}$ in CH_2Cl_2 (blue), CH_3CN, THF, and DMF (red).

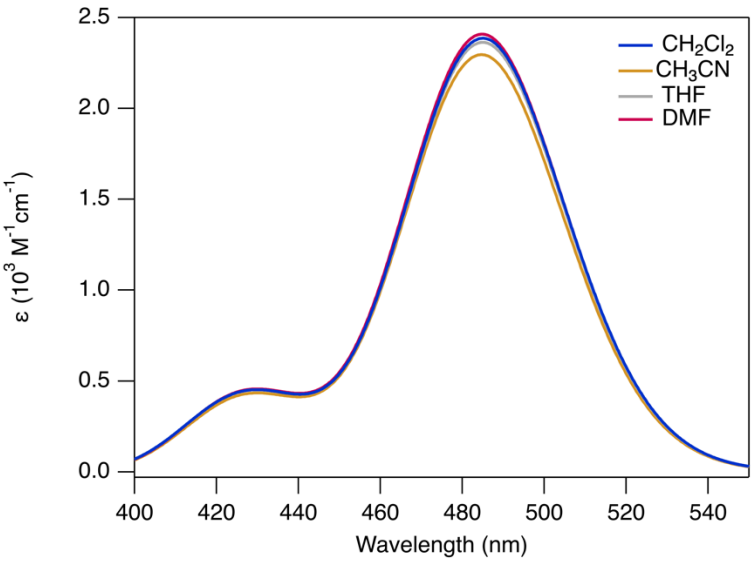

Figure 5: Calculated absorption spectra of $[Re(dmpe)_3]^{2+}$ in CH_2Cl_2, CH_3CN, THF, and DMF using the PCM implicit solvation.

To understand why no solvent-dependence is observed for the LMCT transition in experimental and calculated absorption spectra, dipole moments were calculated for the ground state and the LMCT excited state via single point energy calculations at the DFT and TD-DFT levels of theory, respectively. Minimal differences between the dipole moments of the ground state and the LMCT excited state (state with highest oscillator strength) are observed, with Δμ values ranging from 0.2209 (THF) to 0.2286 (DMF) (Table 1, Table S3). These calculated dipole moments for the ground state and the LMCT excited state support the observed absence of solvatochromism in the absorption spectra of $[Re(dmpe)_3]^{2+}$ (Table S3). The minimal change in dipole moment between the ground and excited state, as well as the orbital fragment Mulliken population analysis described above, reveal that the LMCT excited state is highly delocalized and symmetric—the optical transition observed involves equal electron density moving from all three dmpe ligands to the metal center.

Solvent	Rel. Polarity	λ_{max} (nm)	Δμ* (Debye)
CH_3CN	0.460	527	0.2285
DMF	0.386	531	0.2286
CH_2Cl_2	0.309	526	0.2238
THF	0.207	529	0.2209

Table 1. Reported relative solvent polarities (Reichardt 2003) and absorption band wavelength in respective solvent. Absolute values for computed ground and excited state dipole moments for the lowest-energy LMCT excited state are in SI.

Conclusion

Complexes of the type $[M(dmpe)_3]^{2+}$ (M = Tc, Re) are well-known d^5 complexes that promote room-temperature emission from LMCT excited states. The complex $[Re(dmpe)_3][BAr^F{}_4]_2$ was synthesized following an adapted literature procedure and investigated via UV/Vis absorbance spectroscopy and computational methods. DFT and TD-DFT were used to interrogate the nature of the dominant LMCT transition. Population analysis of the donor and acceptor orbitals reveals a ground state of 82% dmpe (ligand) character and an excited state with 77% Re character. Solvatochromism or solvent-dependent photophysical characteristics can be used to support a charge transfer transition. In the case of $[Re(dmpe)_3]^{2+}$, no solvatochromism was observed across four solvents of different polarities. Computational techniques reveal a symmetric and delocalized LMCT transition, supporting the lack of solvatochromism despite the existence of a charge transfer transition. Solvent effects are important when considering these complexes for their applications as photocatalysts and highly-oxidizing excited states.

Materials and Methods

Computational details and optimized coordinates are included in the Supplementary Information.

Synthesis and characterization

All syntheses were performed under N_2 using standard Schlenk line techniques or in an N_2-filled glovebox unless otherwise noted. All solvents were dried and degassed with argon using a Pure Process Technology solvent system: dichloromethane (Sigma-Aldrich, anhydrous ≥99.8%), diethyl ether (Fisher Scientific, HPLC grade, ≥99%), pentane (Fisher Scientific, HPLC grade, ≥99.9%), and acetonitrile (VWR, ACS reagents). 1,2-dichlorobenzene (Sigma-Aldrich, anhydrous 99%), 1,2-bis(dimethylphosphino)ethane (dmpe) (Sigma-Aldrich, 97%), $[Ph_3C]Cl$ (Sigma-Aldrich, 97%), and $NaBAr^F{}_4$ (Fisher Scientific, 97%) were used without further purification. $[ReO_2(py)_4]Cl$ and $[Ph_3C]BAr^F{}_4$ ($BAr^F{}_4$ = tetrakis[3,5-bis(trifluoromethyl)phenyl]borate) were prepared following reported procedures (Beard et al. 1965; Bahr and Boudjouk 2005). The complexes $[Re(dmpe)_3]BAr^F{}_4$ and $[Re(dmpe)_3](BAr^F{}_4)_2$ were prepared by adapting procedures from literature and described below (Adams et al. 2015).

^1H and $^{31}P\{H\}$ NMR were collected on a Bruker 600 MHz spectrometer at 295K. UV/Visible absorbance spectra were collected with an Agilent Cary 60 UV/vis spectrophotometer.

Adapted Synthesis of $[Re(dmpe)_3]Cl$. $[ReO_2(py)_4]Cl$ (0.683 g, 1.20 mmol), dmpe (1.20 mL, 7.19 mmol), and 20 mL of 1,2-dichlorobenzene were added to a Schlenk flask in an N_2-filled glovebox. The mixture was heated at 170℃ and stirred for 6 h, yielding a dark green solid and light green filtrate. Once cooled, the solid was filtered away under air and the filtrate was kept. Slow addition

of 50 mL of ether to the filtrate yields the product $[Re(dmpe)_3]Cl$ as a white precipitate. Rinsing the white solid with $CHCl_3$ yields pure $[Re(dmpe)_3]Cl$ via NMR (0.709 g, 88% yield).

Synthesis of $[Re(dmpe)_3][BAr^F{}_4]$. The counter anion (Cl^-) was exchanged via salt metathesis by combining the collected product with $NaBAr^F$. $[Re(dmpe)_3]Cl$ (0.368 g, 0.535 mmol) and $NaBAr^F{}_4$ (0.474 g, 0.535 mmol) were dissolved in 35 mL CH_2Cl_2 and stirred at room temperature for 3 h. Excess $NaBAr^F{}_4$ and NaCl were filtered via fine frit inside the glovebox. The filtrate (CH_2Cl_2) volume was reduced to ~ 2 mL under vacuum and 50 mL of MeOH were added to the filtrate to precipitate the product $[Re(dmpe)_3](BAr^F{}_4)$ (0.526 g, 65% yield). ^1H NMR (CD_2Cl_2, 400 MHz) δ 7.72 (t, 8H, $BAr^F{}_4$ H_o and H_m), 7.56 (s, 4H, $BAr^F{}_4$ H_p), 1.65 (m, 6H, $–PCH_2–$), 1.57 (s, 18H, $–P(CH_3)_2$), 1.45 (s, 18H, $–P(CH_3)_2$), 1.41 (m, 6H, $–PCH_2–$).

Synthesis of $[Re(dmpe)_3](BAr^F{}_4)_2$. $[Re(dmpe)_3](BAr^F{}_4)$ (0.20 g, 0.132 mmol) and $[Ph_3C]BAr^F{}_4$ (0.175 g, 0.158 mmol) were dissolved in 10 mL of CH_3CN. Upon mixing, the solution becomes red-orange from a slight reddish solution. The reaction mixture was stirred for 7 h at room temperature and the solvent was removed under vacuum. 15 mL of ether was added to the residue and stirred for 25 min at room temperature. During the 25 min, several color changes were observed from orange, brown, and finally blue with red precipitate product. The red product $[Re(dmpe)_3](BAr^F{}_4)_2$ was collected via filtration (0.125 g, 40% yield). λ_{max} = 527 nm in CH_3CN.

Acknowledgements This work was supported by the National Science Foundation (CHE-1954868). J.L.D. acknowledges support from a Packard Fellowship for Science and Engineering. T.M.R. acknowledges support from the National Science Foundation Graduate Research Fellowship Grant No. DGE-1650116. We thank the University of North Carolina's Department of Chemistry NMR Core Laboratory for the use of their NMR spectrometers. We thank Cole Gruninger and Kelsey Brereton for fruitful discussions and guidance.

References

Adams JJ, Arulsamy N, Sullivan BP, et al (2015) Homoleptic Tris-Diphosphine Re(I) and Re(II) Complexes and Re(II) Photophysics and Photochemistry. Inorg Chem 54:11136–11149. https://doi.org/10.1021/acs.inorgchem.5b01395

Bahr SR, Boudjouk P (2005) Trityl tetrakis[3,5-bis(trifluoromethyl)phenyl]borate: a new hydride abstraction reagent. J Org Chem 57:5545–5547. https://doi.org/10.1021/jo00046a048

Beard JH, Casey J, Murmann RK (1965) The Preparation and Properties of [Re(amine)4O2] + Type Ions. Inorg Chem 4:797–803. https://doi.org/10.1021/ic50028a006

Becke AD (1988) Density-Functional Exchange-Energy Approximation with Correct Asymptotic Behavior. Phys Rev A 38:3098–3100. https://doi.org/10.1063/1.1749835

Becke AD (1993) A new mixing of Hartree-Fock and local density-functional theories. J Chem Phys 98:1372–1377. https://doi.org/10.1063/1.464304

Casida ME, Jamorski C, Casida KC, Salahub DR (1998) Molecular excitation energies to high-lying bound states from time-dependent density-functional response theory: Characterization and correction of the time-dependent local density approximation ionization threshold. J Chem Phys 108:4439–4449. https://doi.org/10.1063/1.475855

Chatterjee S, Negro AS Del, Smith FN, et al (2013) Photophysics and Luminescence Spectroelectrochemistry of [Tc(dmpe) 3] +/2+ (dmpe = 1,2- bis

(dimethylphosphino)ethane). https://doi.org/10.1021/jp406365c
Chen P, Meyer TJ (1998) Medium Effects on Charge Transfer in Metal Complexes. Chem Rev 98:1439–1477. https://doi.org/10.1021/cr941180w
Dolg M, Wedig U, Stoll H, Preuss H (1987) Energy-adjusted ab initio pseudopotentials for the First Row Transition Elements. J Chem Phys 86:866–872
Esswein AJ, Nocera DG (2007) Hydrogen production by molecular photocatalysis. Chem Rev 107:4022–4047. https://doi.org/10.1021/cr050193e
Foo Lee Y, Jon RK (1994) Absorption and luminescence spectroelectrochemical characterization of a highly luminescent rhenium(II) complex. J Am Chem Soc 116:3599–3600. https://doi.org/10.1021/ja00087a056
Gorelsky SI AOMix.pdf. http://www.sg-chem.net/
Hush NS, Reimers JR (2006) Solvent Effects on the Electronic Spectra of Transition Metal Complexes. Chem Commun 100:775–786. https://doi.org/10.1021/cr980409v
Kalyanasundaram K (1982) Photophysics, photochemistry and solar energy conversion with tris(bipyridyl)ruthenium(II) and its analogues. Coord Chem Rev 46:159–244. https://doi.org/10.1016/0010-8545(82)85003-0
Kirchhoff JR, Allen MR, Cheesman B V, et al (1997) Electrochemistry and spectroelectrochemistry of [Re (1 , 2-bis (dimethylphosphino) ethane) 3] q. Inorganica Chim Acta 262:195–202
Krishnan R, Binkley JS, Seeger R, Pople JA (1980) Self-consistent molecular orbital methods. XX. A basis set for correlated wave functions. J Chem Phys 72:650–654. https://doi.org/10.1063/1.438955
Loukova G V., Huhn W, Vasiliev VP, Smirnov VA (2007a) Ligand-to-metal charge transfer excited states with unprecedented luminescence yield in fluid solution. J Phys Chem A 111:4117–4121. https://doi.org/10.1021/jp0721797
Loukova G V., Huhn W, Vasiliev VP, Smirnov VA (2007b) Ligand-to-metal charge transfer excited states with unprecedented luminescence yield in fluid solution. J Phys Chem A 111:4117–4121. https://doi.org/10.1021/jp0721797
Loukova G V., Milov AA, Vasiliev VP, Minkin VI (2016) Dipole moments and solvatochromism of metal complexes: Principle photophysical and theoretical approach. Phys Chem Chem Phys 18:17822–17826. https://doi.org/10.1039/c6cp03348b
Marini A, Muñoz-losa A, Biancardi A, Mennucci B (2010) What is solvatochromism? J Phys Chem B 114:17128–17135
McLean AD, Chandler GS (1980) Contracted Gaussian basis sets for molecular calculations. I. Second row atoms, Z=11-18. J Chem Phys 72:5639–5648. https://doi.org/10.1063/1.438980
Negro AS Del, Seliskar CJ, Heineman WR, et al (2006a) Highly Oxidizing Excited States of Re and Tc Complexes. J Am Chem Soc 128:16494–16495. https://doi.org/10.1021/ja067114g
Negro AS Del, Sullivan BP, Negro D (2006b) Highly Oxidizing Excited States of Transition Metal Complexes. J Am Chem Soc 128:16494–16495
Paulson S, Sullivan BP, Caspar J V. (1992) Luminescent Ligand-to-Metal Charge-Transfer Excited States Based on Pentamethylcyclopentadienyl Complexes of Tantalum. J Am Chem Soc 114:6905–6906. https://doi.org/10.1021/ja00043a040
Prier CK, Rankic DA, MacMillan DWC (2013) Visible light photoredox catalysis with transition metal complexes: Applications in organic synthesis. Chem Rev 113:5322–5363. https://doi.org/10.1021/cr300503r
Reichardt C (1994) Solvatochromic Dyes as Solvent Polarity Indicators. Chem Rev 94:2319–

2358
Reichardt C (2003) Reichardt - Solvents in Organic Synthesis. In: Solvents and Solvent Effects in Organic Chemistry, 3rd edn. Wiley-VCH Publishers
Scalmani G, Frisch MJ (2010) Continuous surface charge polarizable continuum models of solvation. I. General formalism. J Chem Phys 132:. https://doi.org/10.1063/1.3359469
Shepherd RE, Hoq MF, Hoblack N, Johnson CR (1984) Solvatochromism of the LMCT Transition of Pentacyanoferrate(III) Complexes. Inorg Chem 23:3249–3252. https://doi.org/10.1021/ic00188a043
Sullivan BP (1989) Large solvatochromism of metal-to-ligand charge-transfer transitions in organometallic complexes of Re(I). J Phys Chem 93:24–26. https://doi.org/10.1021/j100338a009
Zhang Y, Lee TS, Favale JM, et al (2020) Delayed fluorescence from a zirconium(iv) photosensitizer with ligand-to-metal charge-transfer excited states. Nat Chem 12:345–352. https://doi.org/10.1038/s41557-020-0430-7